Journal of
Nanoscience and Nanotechnology
Vol. 11, 5440–5445, 2011

Strontium Doped Lead Zirconate Titanate Ceramics: Study of Calcination and Sintering Process to Improve Piezo Effect

Muhammad Khalid[1], Muhammad Shoaib[2], and Amir Azam Khan[3,*]

[1] *School of Chemical and Materials Engineering (SCME),*
National University of Sciences and Technology (NUST), Sector H 12, Islamabad 44000, Pakistan
[2] *Department of Materials Engineering, Institute of Space Technology (IST), Islamabad 44000, Pakistan*
[3] *Department of Mechanical and Manufacturing Engineering, Universiti Malaysia Sarawak (UNIMAS),*
94300 Kota Samarahan, Sarawak, Malaysia

Perovskite crystal structure is found in many ionic solids like $CaTiO_3$, $BaTiO_3$ and Lead Zirconate Titanates (PZT). In this structure off-center position of cations in oxygen octahedral causes polarization and produces direct and indirect piezoelectric responses in ceramic materials that are suitable for many ultrasonic applications. In the present study 9% Sr doped PZT ceramics were prepared and their dielectric and piezoelectric properties measured. X ray Diffraction (XRD) analysis of calcined powders demonstrated a decrease in the PbO content during the calcination stage at 850 °C. This was counterbalanced by adding excess PbO at the time of preparation of mixtures. Sintering was carried out at 1200 °C for 2 hours in lead rich atmosphere. The properties achieved were Dielectric Constant $(K) = 1440$, Tangent Loss $(\tan\delta) = 0.0062$, Charge Coefficient $(d_{33}) = 335$ pC/N and density $= 7.55$ g/cm^3. SEM analysis of sintered samples demonstrated that grain size was 2–3 μm with clean grain boundaries and no large size porosity observed. XRD analysis of sintered pellets exhibited that material prepared was free of any precipitated phase usually harmful for the piezo effect.

Keywords: Lead Zirconate Titanate (PZT), Strontium, Doping, Sintering, Piezo-Electric Effect.

1. INTRODUCTION

Despite years of research for a lead-free alternative, the solid solution of Lead Zirconate and Lead Titanate $Pb(Zr_xTi_{1-x})O_3$ remains the most widely used ceramic system for piezoelectric applications.[1] The piezoelectric coefficients and electromechanical coupling factors of these materials are enhanced at compositions near the morphotropic phase boundary $x \approx 0.53$ which separate rhombohedral and tetragonal phases.[2] Further improvements in some of the piezoelectric properties are achieved through off valence and isovalent substitutions near the Morphotropic Phase Boundary (MPH).[3–6] Off valence (or aliovalent) substitutions such as Nb^{5+} replacing Zr^{4+} or La^{3+} replacing Pb^{2+} are designated as donor (soft) dopants while additives such as Fe^{3+} replacing Zr^{4+} or K^+ replacing Pb^{2+} are called acceptor (hard) dopants. Donor dopants are characterized by square hysteresis loop, low coercivity, high remnant polarization, high electrical resistivity, high dielectric constant, high dielectric loss and reduced aging.[3–6] Acceptor dopants are characterized by poorly developed hysteresis loops, lower dielectric constant, low dielectric loss and high aging rates.[3–6] Isovalent additives, such as Ba^{2+} or Sr^{2+} replacing Pb^{2+} or Sn^{4+} replacing Zr^{4+} or Ti^{4+}, in which the substituting ion is of the same valency and approximately the same size as the replaced ion. Solid solution ranges with these additives are usually quite extensive and result in lower curie points and increase dielectric constant, poorly developed hysteresis loops, lower dielectric loss and higher aging rates.[3–6] Present work focuses on processing and piezoelectric properties in 9 mol% Sr doped PZTs. Strontium is an isovalent substituent. The effects of Sr substitution in PZT have been studied by researchers previously. It has been found that Sr substitution lowers the Curie point (Tc) which enhances the permittivity and also results in enhancement of d_{33}.[2,6] For every 1 atomic % addition there is 9 °C decrease in Curie point.[2] In Nb doped PZT ceramics, Sr substitution up to 32 mol% decreases Tc from 360 to 30 °C.[7]

---

[*] Author to whom correspondence should be addressed.

1533-4880/2011/11/5440/006 doi:10.1166/jnn.2011.3791

In addition to decreasing Tc, Sr broadens the phase transition maximum implying that the distribution of Curie temperature is increased.[7] The role of Sr addition to increase d_{33} has been addressed at length in studies.[7,8] It has been demonstrated in a previous study[7] that in Nb doped PZT, the addition of Sr up to 16 mol% continuously decrease d_{33} for Zr:Ti ratio of 1.095. The study[7] has shown that for optimization of d_{33}, Zr:Ti ratio is an important factor. Since Sr doping in PZTs promotes the tetragonal over the rhombohedral[7] phase for a fixed Zr:Ti ratio, to optimize d_{33} Zr:Ti ratio has to be increased to achieve composition near MPB. In other study[8] with enhanced Zr:Ti ratio, the research has shown that d_{33} first increases upto 12 mol% addition of Sr to PZT solid solution and then exhibit decreasing trend. Following the above discussion it is clear that role of Sr addition to PZT to enhance d_{33} requires further investigation.

PZT compositions with 6 mole% Sr have been studied extensively[2,9,10] but compositions with higher Sr concentrations (without Nb or Sb addition) are rarely worked out. A systematic study in manufacturing of PZT ceramics with higher Sr concentration (>6 mol%) prepared from conventional mixed oxide route is still lacking. The purpose of present work is to assess the influence of higher Sr doping (9 mol%) on dielectric and piezoelectric properties in PZTs and examine the changes occurring in microstructure and homogeneity as the manufacturing process proceeds from initial stage of mixing to calcination to final stage of sintering.

2. EXPERIMENTAL WORK

PZT samples with 9 mole% Sr doping were prepared by mixing of oxides such as PbO, TiO_2, ZrO_2 and $SrCO_3$, according to the formulae $Pb_{0.91}Sr_{0.09}(Zr_{0.53},Ti_{0.47})O_3$ with 2.5 wt% excess PbO to account for lead loss during calcination and densification. The purity of precursor powders is as follows: PbO $> 99\%$ (Fluka, Switzerland), TiO_2 $> 99\%$ (Riedel-de-Haén® Germany), ZrO_2 and $SrCO_3$ $> 99\%$ (Alpha Aesar).

Starting powders were analyzed for particle size through Laser Particle Size Analyzer (Horiba LA 920) and then mixed in appropriate ratios under wet conditions (with isopropanol) in a planetary mill for 11 hours at 100 rpm. The rotation direction was reversed after 15 minute to get a thorough mixing. Mixing was carried out in 250 ml WC bowls using zirconia balls as grinding media. After mixing the powders were dried at 70 °C for 24 hours. Dried powder was pressed at 100 MPa in the shape of disc of size diameter 25 mm × 10 mm thickness and calcined at 850 °C for 2 to 15 hours in alumina crucibles covered with lid. Heating rate was kept at 3 °C/min followed by furnace cooling. Calcined powder was ground and then characterized by XRD for perovskite phase formation and by SEM analysis for grain size and morphology. Calcined powder was mixed with 2% PVA binder in a planetary mill for 4 hours and then dried at 70 °C. The powder was then passed through 150 μm sieve. Pellets of size, OD 13 mm, ID 04 mm and thickness 5 mm, were pressed at 180 MPa. After that samples were heated to 600 °C at a rate of 2 °C/min and hold for 4 hours to ensure complete removal of organic binder. After debinding the samples were sintered at 1200 °C for 2 hours in sealed alumina crucibles. Heating and cooling rate was maintained at 3 °C/min. Pellets were surrounded by Pb rich powder to avoid PbO loss. Sealing was carried out by mixture of fine alumina powder and sodium silicate. Sintered pellets were metallized using silver conductor (ESL 599-E) purchased from Electro-Science Laboratories, Inc., USA. A silver coating in the form of paste was applied to samples using 325 mesh silk sieve. Pellets were dried with air heater at 100 °C for 10 minutes and then fired at 550 °C for 15 minutes with ascent/descent rate of 60 °C/min. Pellets were poled at 15 KV (3.5 KV/mm) in silicon oil at 110 °C for 20 minutes. Dielectric properties were measured using Precision LCR meter at 1 KHz. Charge coefficient, d_{33}, was measured by Piezometer at a frequency of 110 Hz. Static force (about 10 N) was employed to clamp the test piece within the jaws while an oscillating force of 0.25 N used for measuring d_{33} coefficient. Particle size and shape was characterized by SEM analysis (Jeol JSM 5910 LV Japan at 20 KV) and the crystal structures of calcined and sintered samples were determined using XRD equipment (Stoe Theta-Theta Diffractometer System STAD I Germany) using Cu Kα as radiation source and Ni as filter. Particle size analysis was made by Laser Particle Size Analyzer, Model LA-920 Horiba, Japan. This instrument can measure in the range 20 nm to 2 mm.

3. RESULTS AND DISCUSSION

3.1. Particle Size Analysis

The precursor powders were characterized in terms of particle size and size distribution by laser particle size and results are shown in the Figure 1. In this figure it is shown that PbO has bimodal particle size distribution In this distribution 30% of particles lie in the range of 0.3–1 μm and 70% lie in 1–10 μm range and mean size is 3.10 μm. ZrO_2 has mean particle size of 0.52 μm and TiO_2 is 0.18 μm. $SrCO_3$ powder has multimode particle size distribution (0.2–10 μm) with mean particle size of 1.6 μm.

3.2. Mixing and Grinding of Powders

The precursor powders (PbO, TiO_2, ZrO_2, $SrCO_3$) were wet mixed with isopropanol in a planetary mill for 11 hours. Planetary mill not only mixes the precursor powders but also results in reduction of particle size. Particle size distribution after mixing is shown in Figure 2.

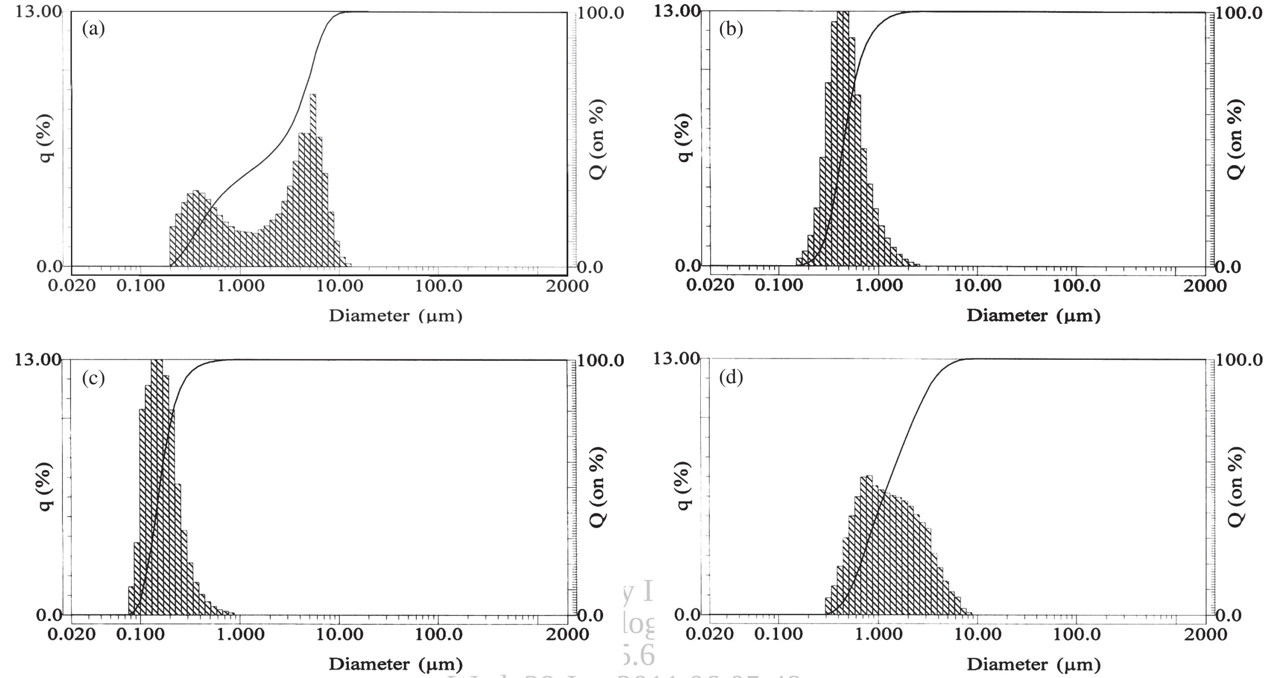

Fig. 1. Laser particle size analysis of precursor powders (a) PbO (b) ZrO_2 (c) TiO_2 (d) $SrCO_3$.

In this figure it is seen that about 10% of particles are in the range of 1 μm to 10 μm while about 90% of particles are less than 1 μm. It is presumed that most of the large particle sizes (1 μm to 10 μm) present initially in PbO and $SrCO_3$ precursor powder has been reduced to finer size (<1 μm) in the process of milling while some large particle sizes of these powders are still present in the mixture after milling.

3.3. Calcination

3.3.1. SEM Analysis

Calcination was carried out at 850 °C for 2, 8 and 15 hours. SEM profiles of calcined powders are shown in the Figures 3(a–d). Figure 3(d) shows higher magnification picture of the powder calcined for 15 hours. It shows formation of necks between the particles. Formation of necks at this stage may be attributed to presence of liquid (PbO rich) phase at the calcination temperature (850 °C). SEM micrographs in Figures 3(a–c) also show skeletal type structure after calcination. This structure is due to the fact that the formation of PZT (perovskite structure) is accompanied by volume expansion, PZT phase having different molar volume than its component oxides. The formation of PZT from its component oxides requires that the perovskite formation reaction should be complete prior to the sintering step since further morphological changes may hinder densification and overall homogeneity of the product.

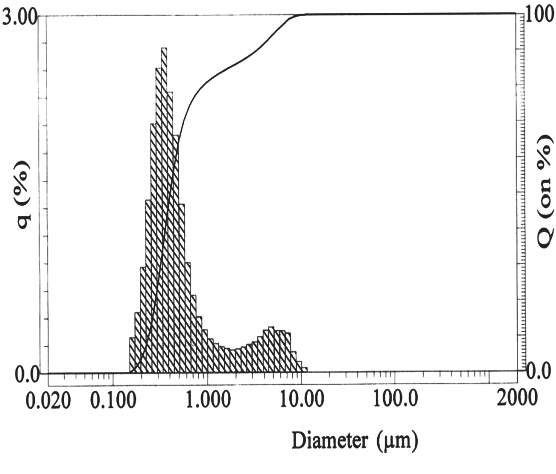

Fig. 2. Particle size distribution of mixed powder by laser particle size analyzer.

3.3.2. XRD Analysis

The calcined samples were subjected to XRD analysis to ensure complete formation of PZT phase (perovskite structure) and the detection of unwanted phases such as ZrO_2, PbO and PbO_{ss}. The XRD pattern for 2 hours calcination at 850 °C is shown in the Figure 4. The pattern was matched with ICDD card *01-070-4265*, $Pb(Zr_{0.53}Ti_{0.47})O_3$, which shows a rhombohedral symmetry. Except a small PbO peak at $2\theta = 29°$ all the peaks matches to this card which shows the structure is mainly perovskite. Emergence of PbO peaks indicates that some unreacted or extra PbO added is present after 2 hours of calcination. Similar XRD patterns for samples calcined at 8 and 15 hours are shown in the Figures 5 and 6 respectively. After 8 hours of calcination the intensity of PbO peak gets reduced

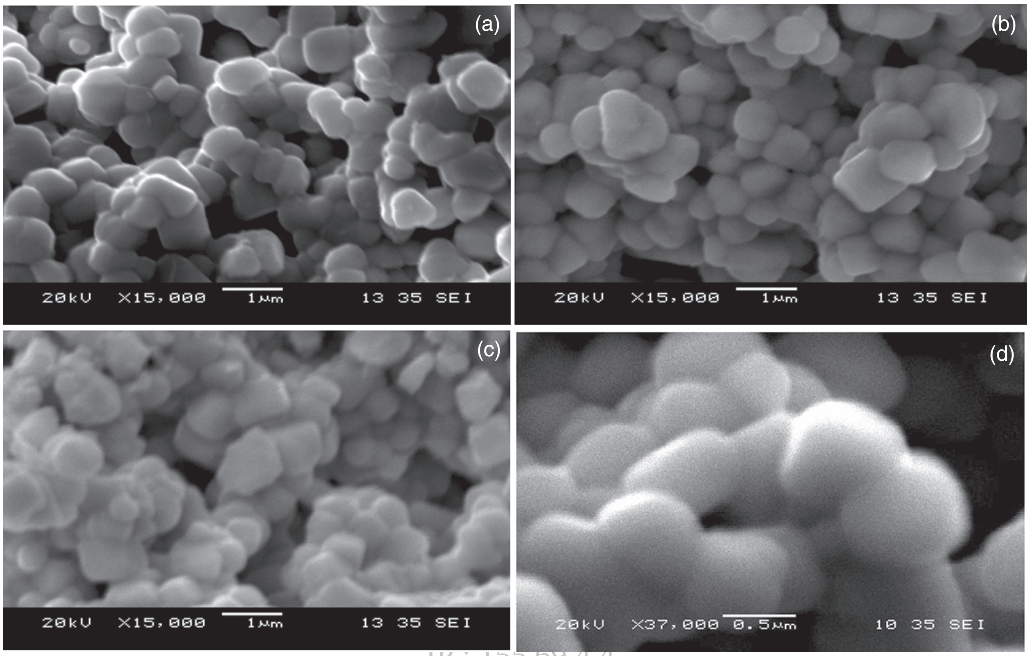

Fig. 3. SEM micrographs after calcination of precursor powders: (a) 2 hours (b) 8 hours (c) 15 hours (d) Same as (c) but at higher magnification.

indicating that some PbO has evaporated or dissolved into PZT phase. When the sample was calcined for 15 hours PbO phase is not observed in XRD pattern as shown in the Figure 6. After calcination at 850 °C for 15 hours it is assumed that all of the excess PbO added has evaporated or dissolved in perovskite phase. One more trend that is observed is that intensities of the peaks increased gradually as holding time increased. The intensity of the reflection for plane (110) is 900, 1040 and 1200 for 2 hours, 8 hours and 15 hours calcination at 850 °C. The increase in peak intensity is attributed to some initial sintering occurring at this temperature due to presence of liquid phase (PbO). Melting of PbO starts at 800 °C.[12] Presence of liquid phase at this temperature causes some necking between the grains and the grain boundary area starts decreasing. Because grain boundaries are considered as amorphous areas, the intensities of XRD reflections will increase slightly when the grain boundary areas decrease. The other possible reason for increase in intensity of major XRD peak is that as the holding time is being increased during calcination, compositional homogenization is also taking place that result in increase in intensity of peaks.

All the XRD patterns show peak broadening. The same type of broadened peaks after calcination are observed in the work of Shue-Sheng and collaborators.[13] Peak broadening decreases when the samples are sintered as shown in the Figure 7. This peak broadening may be attributed to compositional fluctuation in the solid solution and it will be discussed later in Section 3.4.

3.4. Sintering

3.4.1. SEM Analysis

Sintering was carried out in lead rich atmosphere to avoid loss of PbO. The sintering temperature was kept at 1200 °C and sintering dwell time was 2 hours. Only powder samples that were calcined at 850 °C for 15 hours, were sintered. SEM micrographs of sintered samples taken at different magnifications are shown in Figure 7. At higher

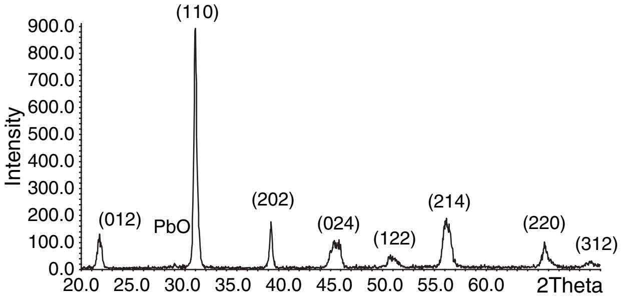

Fig. 4. XRD pattern after 2 hours of calcination at 850 °C.

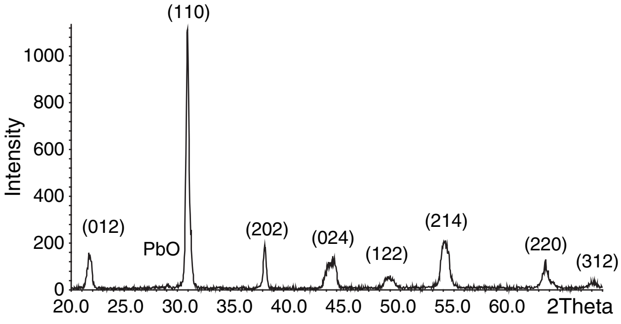

Fig. 5. XRD pattern after 8 hours of calcination at 850 °C.

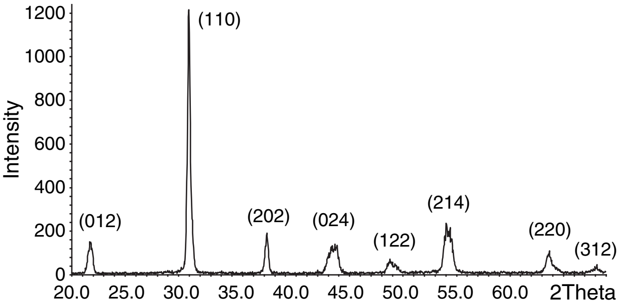

Fig. 6. XRD pattern after 15 hours of calcination at 850 °C.

magnification (Figs. 7(c) and (d)) a dense microstructure is achieved. Figure 7(a) shows polished surface of sintered sample at low magnification. Some porosity in the sample is observed in this micrograph but the size of porosity is less than or equal to grain size (2–3 μm). Porosity less than or close to the grain size is a normal feature in sintered parts in PZTs prepared by conventional slow heating cycle. SEM analysis of sintered and fractured samples reveal the morphology of grain and mode of fracture, as shown in Figures 7(b–d). These SEM micrographs of the fractured surface of sintered samples are taken at different magnifications and locations. It can be seen in the Figure 7(d) that the grain surfaces are very clean and no observable secondary phase is present at the grain boundaries. The mode of fracture is mixed. Grain size is about 2–3 μm and no abnormal grain growth is seen. Size of the grains is more or less uniform.

3.4.2. XRD Analysis

Sintered and poled pellets were ground to powder by mortar and pestle and were subjected to XRD analysis. XRD pattern is shown in Figure 8. All the peaks correspond to PZT perovskite phase. Compared to XRD patterns in calcined condition (Figs. 4–6) it is observed that broadened peaks of the planes (024), (122) and (214) in the calcined condition are replaced by two distinct peaks for each set of planes. Emergence of extra peaks in the sintered condition (Fig. 8) is due to better homogenization of structure at sintering temperature (1200 °C). It may also be attributed to removal of stresses and defects induced by milling of PZT powder in a planetary mill. Usually the sintering process enhances the electrical response of the ferroelectric ceramic via promotion of the ferroelectric phase and by increasing crystallanity. The XRD patterns after calcination (Figs. 4–6) match to ICDD card 01-070-4265 which shows a rhombohedral symmetry while after sintering the XRD pattern (Fig. 8) matches to card 01-072-7169 which gives tetragonal symmetry. Sub-stoichometric PbO concentration shift (possible during sintering) causes precipitation of ZrO_2 from PZT solid solution.[2,8] This decomposition renders the solid solution towards $PbTiO_3$ side of MPB in $PbZrO_3$-$PbTiO_3$ system which has tetragonal symmetry and hence the net effect in the XRD pattern

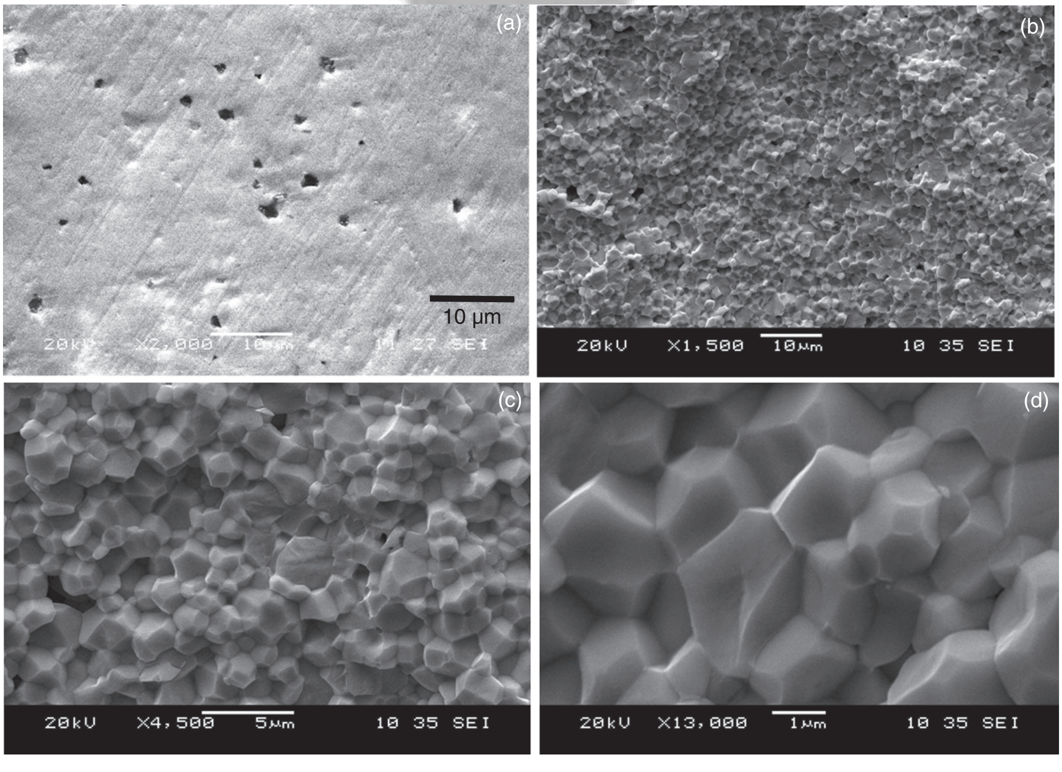

Fig. 7. SEM micrographs after sintering (a) Polished surface (b) Fractured surface (c) Fractured surface (d) Fractured surface.

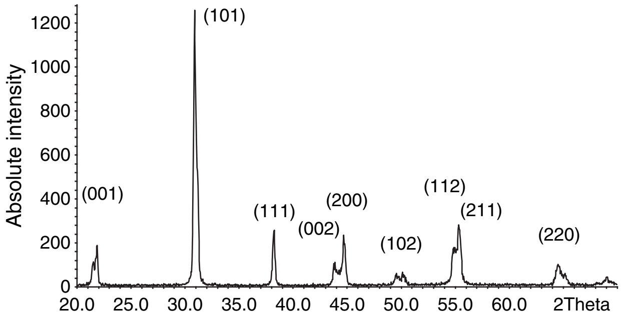

Fig. 8. XRD pattern for sintered, poled and ground PZT sample.

(Fig. 8) can be explained. To ascertain the deficiency of PbO in the sintered sample EDX analysis was carried out. The EDX analysis result exhibited 2.5 atomic % less Pb than the stoichometric amount.

3.5. Dielectric and Piezoelectric Properties

Sintered pellets were poled at 3.5 KV/mm in silicon oil at 110 °C. In the present work (9 mol% doped PZT) the properties achieved are Dielectric Costant $(K) = 1440$, Tangent Loss $(\tan\delta) = 0.0062$, Charge Coefficient $(d_{33}) = 335$ pC/N, and Density $= 7.55$ g/cm^3. The reported values[2, 6, 9, 10] for 6 mol% Sr doped PZTs are Dielectric Cosntant $(K) = 1300$, Tangent Loss $(\tan\delta) = 0.004$, Charge Coefficient $(d_{33}) = 289$ pC/N. Therefore, by increasing Sr content in PZTs higher values of dielectric and piezoelectric constants are achieved with accompanying increase in dielectric loss.

4. CONCLUSION

Lead Zirconate Titanate (PZT) with a stoichometry of $Pb_{0.91}Sr_{0.09}(Zr_{0.53}Ti_{0.47})O_3$ was prepared by conventional mixed oxide route. XRD after mixing and calcination of the starting powders show that formation of PZT is complete after calcination at 850 °C, for two hours. Calcination for longer times improves the intensity of the peaks, which correlates to growth in the crystallite sizes. Properties achieved by sintering at 1200 °C for 2 hours in lead rich atmosphere were Dielectric Cosntant $(K) = 1440$, Tangent Loss $(\tan\delta) = 0.0062$, Charge Coefficient $(d_{33}) = 335$ pC/N, and density $= 7.55$ g/cm^3. An isovalent substituted PZT with 9 mol% Sr (present study) gives higher values of dielectric constant and charge coefficient (d_{33}) than the reported values for a strontium doped PZT with 6 mol% Sr doping.[2, 6, 9, 10] Sintered pellets show a very dense microstructure with grain size of 2–3 μm after sintering at 1200 °C for 2 hours.

References and Notes

1. N. J. Donnelly, T. R. Shrout, and C. A. Randall, *J. Am. Ceram. Soc.* 90, 490 (**2007**).
2. B. Jaffe, W. R. Cook, and H. Jaffe, Piezoelectric Ceramics, Academic Press, New York (**1971**).
3. D. Berlincourt, *J. Acoust. Soc. Am.* 91, 3034 (**1992**).
4. G. Goodman, Ceramic Materials for Electronics, edited by R. C. Buchanan, Marcel Dekker, New York (**1986**), p. 79.
5. C. A. Harper, Electronic Materials and Process Handbook, 3rd edn., McGraw-Hill (**2004**).
6. H. Banno, The Encyclopaedia of Advanced Materials edited by D. Bloor, R. J. Brook, M. C. Fleming, and S. Mohajan, Elsevier Science, UK (**1994**), Vol. 3, p. 2017.
7. H. Zheng, I. M. Reaney, W. E. Lee, N. Jones, and H. Thomas, *J. Europ. Ceram. Soc.* 21, 1371 (**2001**).
8. H. Zheng, I. M. Reaney, W. E. Lee, N. Jones, and H. Thomas, *J. Amer. Ceram. Soc.* 85, 2337 (**2002**).
9. S. Sirilomask, W. A. Schulze, S. M. Pilgrim, and F. A. William, Jr., *J. Amer. Ceram. Soc.* 88, 2121 (**2005**).
10. C. A. Randall, N. Kim, J. Kucera, W. Cao, and T. R. Shrout, *J. Am. Ceram. Soc.* 81, 677 (**1998**).
11. T. R Shrout, P. Papet, S. Kim, and G.-S. Lee, *J. Amer. Ceram. Soc.* 73, 1862 (**1990**).
12. A. J. Moulson and J. M. Herbert, Electroceramics Materials: Properties, Applications, 2nd edn., John Wiley and Sons, Sussex, England (**2003**).
13. S.-S. Chiang, M. Nishioka, R. M. Fulrath, and J. A. Pask, *Ceramic Bulletin* 60, 484 (**1981**).

Received: 14 August 2009. Accepted: 1 March 2010.